

## Observation of ambipolar field-effect behavior in donor–acceptor conjugated copolymers†

Shinuk Cho,<sup>\*a</sup> Jung Hwa Seo,<sup>b</sup> Gi-Hwan Kim,<sup>c</sup> Jin Young Kim<sup>\*c</sup> and Han Young Woo<sup>d</sup>

Received 24th July 2012, Accepted 23rd August 2012

DOI: 10.1039/c2jm34872a

Although donor (D)–acceptor (A) conjugated copolymers possess an electron deficient unit, most D–A copolymers exhibit only hole transport properties (p-type). While there are some D–A copolymers that show ambipolarity, n-type behaviour is highly dependent on the type of acceptor used. In this work, ambipolar field-effect behaviour was derived from general D–A conjugated copolymers, believed to be a typical p-type material, by introducing a functional passivation layer between gate dielectric and active layers using polypropylene-*co*-1-butene (PPcB). The PPcB layer effectively covered the hydroxyl groups and induced a reduction in the energetic disorder at the semiconductor–insulator interface. As a result, the FET devices fabricated using D–A conjugated copolymers, such as PCDTBT, PTBT and Si-PCPDTBT, showed clear ambipolar properties.

## Introduction

Conjugated copolymers with electron donor (D)–acceptor (A) units in the repeat unit have drawn considerable attention for bulk heterojunction photovoltaic (PV) cells because their intramolecular charge transfer (ICT) from the electron-donating segments to the electron-accepting segments can lead to low-band-gap conjugated polymers that enable efficient harvesting of the solar spectrum.<sup>1–8</sup> In addition, because they exhibit relatively high mobilities, such D–A conjugated copolymers are also of interest for use as the active materials in polymer field-effect transistors (pFETs).<sup>8–11</sup>

Since the D–A conjugated copolymers possess an electron deficient unit (electron acceptor), they are expected to have ambipolar behavior. However, most D–A copolymers, particularly of the DDAD type, which have the most popular structure (for example, donor–thiophene–acceptor–thiophene), exhibit only hole transport properties (p-type).<sup>8–15</sup> It is generally believed that the main reason for the absence of n-type behavior is

electron localization in the electron deficient unit. While there are some D–A copolymers that show ambipolarity,<sup>16–19</sup> n-type behavior is highly dependent on the type of acceptor used.

In addition, there have been several reports emphasizing the importance of the gate dielectric in organic field-effect transistors (FETs). Particularly, for organic n-type FETs, selection of the gate dielectric is more important because the n-type property is strongly influenced by the surface properties of gate dielectrics. In the case of the commonly used SiO<sub>2</sub> dielectric, for example, hydroxyl groups at the dielectric interface trap electrons, making n-type behavior elusive.<sup>20</sup>

In this work, we derived ambipolar field-effect behavior from general D–A conjugated copolymers, believed to be a typical p-type material, by introducing a functional passivation layer between the gate dielectric layer and the active layer using polypropylene-*co*-1-butene (PPcB). Beyond the function of a simple passivation layer to remove hydroxyl groups, which act as trap sites for electrons, the PPcB layer induced a lower energetic disorder at the semiconductor–insulator interface. Therefore, the FETs fabricated using D–A copolymers showed clear ambipolar properties.

## Experimental section

## Fabrication and characterizations of FET devices

All transistors were fabricated in the bottom gate, top contact configuration on heavily doped n-type Si substrates as the gate and thermally grown SiO<sub>2</sub> (200 nm) as the dielectric layer.

The semiconducting layer was spin-cast from solution at 2500 rpm. All solutions were prepared at a concentration of 5 mg mL<sup>-1</sup> in chlorobenzene. Prior to the deposition of D–A conjugated copolymers, the SiO<sub>2</sub> surface was modified with

<sup>a</sup>Department of Physics and EHSRC, University of Ulsan, Ulsan 680-749, Republic of Korea. E-mail: [sucho@ulsan.ac.kr](mailto:sucho@ulsan.ac.kr); Fax: +82 52 259 1693; Tel: +82 52 259 1268

<sup>b</sup>Department of Materials Physics, Dong-A University, Busan 604-714, Republic of Korea

<sup>c</sup>Interdisciplinary School of Green Energy, Ulsan National Institute of Science and Technology, Ulsan 689-798, Republic of Korea. E-mail: [jykim@unist.ac.kr](mailto:jykim@unist.ac.kr)

<sup>d</sup>Department of Nanofusion Technology and Cogno-Mechanics Engineering, Pusan National University, Miryang 627-706, Republic of Korea

† Electronic supplementary information (ESI) available: AFM topology images of PPcB and PCDTBT on PPcB, FET results obtained from a PTBT FET fabricated on an OTS-treated SiO<sub>2</sub> substrate, and output characteristics of ambipolar PTBT and Si-PCPDTBT FETs. See DOI: 10.1039/c2jm34872a

polypropylene-*co*-1-butene (PPcB). PPcB (20 mg) was dissolved in 1.0 mL decahydronaphthalene at 200 °C.

After PPcB layer deposition, the substrate was subsequently dried on a hot plate stabilized at 190 °C for 10 minutes. After polymer deposition, the films were dried on a hot plate stabilized at 80 °C for 30 minutes. All polymer deposition processes were carried out in a controlled atmosphere glove box filled with N<sub>2</sub>.

Source and drain electrodes were deposited by thermal evaporation using a shadow mask. The thickness of the source and drain electrodes was 70 nm. The channel length (*L*) and channel width (*W*) were 50 μm and 2.5 mm, respectively. Electrical characterization was performed under N<sub>2</sub> atmosphere using a Keithley semiconductor parametric analyzer (Keithley 4200).

### Ultraviolet photoelectron spectroscopy (UPS)

For UPS experiments, 80 nm thick Au films were deposited on pre-cleaned Si wafers with a thin native oxide. PCDTBT layers were then spin-cast from chlorobenzene onto the Au and PPcB layers. Films were fabricated in a N<sub>2</sub> atmosphere. To minimize the possible influence of exposure to air, the films were then transferred from the N<sub>2</sub>-atmosphere dry box to the analysis chamber inside an air-free sample holder. Subsequently, all samples were kept inside a high-vacuum chamber overnight to remove any residual solvent.

The UPS analysis chamber was equipped with a hemispherical electron energy analyzer (Kratos Ultra Spectrometer) and maintained at  $1 \times 10^{-9}$  Torr. The UPS measurements were taken using a He I (*hν* = 21.2 eV) source. The electron energy analyzer was operated at a constant pass energy of 10 eV. A sample bias of -9 V was used during UPS measurements in order to separate the sample and the secondary edge for the analyzer.

### Results and discussion

Fig. 1a shows the chemical structures of the D–A conjugated copolymer and PPcB used in this study. A typical DDAD-type D–A copolymer, poly[*N*-9'-hepta-decanyl-2,7-carbazole-*alt*-5,5-(4',7'-di-2-thienyl-2',1',3'-benzothiadiazole)] (PCDTBT), which is believed to be a p-type material,<sup>3,9</sup> was initially tested. Fig. 1b is a schematic of the device structures of PCDTBT FET fabricated on a SiO<sub>2</sub> (200 nm)/n<sup>++</sup> Si substrate covered by a 50 nm thick layer of spun-cast PPcB containing 14 wt% 1-butene. PPcB was obtained from Aldrich and used as received without any further treatment. PPcB (20 mg) was dissolved in 1.0 mL decahydronaphthalene at 200 °C. After PPcB layer deposition using hot solution, the substrate was subsequently dried on a hot plate stabilized at 190 °C for 10 min. The capacitance measured for the PPcB/SiO<sub>2</sub> gate dielectric was 8.5 nF cm<sup>-2</sup>. The semiconducting PCDTBT layer was spin-cast from solution at 3000 rpm in a controlled atmosphere glove box filled with N<sub>2</sub>.

Fig. 2 shows the transport characteristic curves, *I*<sub>ds</sub> versus *V*<sub>gs</sub> (ds = drain source, gs = gate source), of PCDTBT FET fabricated on octyltrichlorosilane (OTS)-treated SiO<sub>2</sub> and PPcB-modified SiO<sub>2</sub>. PCDTBT FETs were fabricated on a heavily doped n-type Si wafer with a 200 nm thick, thermally grown SiO<sub>2</sub> layer with top contact geometry. The channel length (*L*) and the channel width (*W*) were *L* = 50 μm and *W* = 2500 μm, respectively.

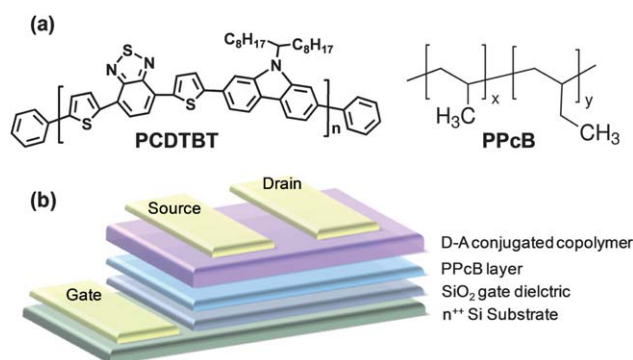


**Fig. 1** (a) Chemical structures of PCDTBT and PPcB. (b) Schematic of the FET device structure.

*I*<sub>ds</sub>–*V*<sub>gs</sub> curves obtained from PCDTBT on OTS-treated SiO<sub>2</sub> were typical of p-type semiconductors, as reported previously.<sup>9</sup> Linear plots of *I*<sub>ds</sub><sup>1/2</sup>–*V*<sub>gs</sub>, deduced from the *I*<sub>ds</sub>–*V*<sub>gs</sub> measurements, yielded hole mobilities of  $1.2 \times 10^{-2}$  cm<sup>2</sup> V<sup>-1</sup> s<sup>-1</sup>. However, for the PCDTBT FET fabricated on PPcB-modified SiO<sub>2</sub>, although very weak electron transport was observed, the FET device clearly exhibited typical bipolar FET characteristics, which included v-shape transport characteristic curves in both p-type operation (*V*<sub>gs</sub> < 0, *V*<sub>ds</sub> < 0) and n-type operation (*V*<sub>gs</sub> > 0, *V*<sub>ds</sub> > 0).

Since we used gold metal (Au) as the source and drain electrodes, there may have been some difficulty with electron injection into the lowest unoccupied molecular orbital (LUMO) of PCDTBT because of the big energy barrier. In order to enhance the electron injection, we introduced an electron injection layer at the interface between the electrode and the PCDTBT layer using conjugated polyelectrolyte, Blm4.<sup>21,22</sup> The result clearly shows enhanced n-type behavior. PCDTBT ambipolar FETs exhibited the highest hole and electron mobilities of  $3.1 \times 10^{-3}$  cm<sup>2</sup> V<sup>-1</sup> s<sup>-1</sup> and  $5.8 \times 10^{-4}$  cm<sup>2</sup> V<sup>-1</sup> s<sup>-1</sup>, respectively.

Fig. 3 shows the output characteristic curves (*I*<sub>ds</sub>–*V*<sub>ds</sub>) of PCDTBT FETs with and without the PPcB layer. The PCDTBT FET without the PPcB layer showed only p-type output characteristics. However, the output characteristic curves of the PCDTBT FET with the PPcB layer showed typical ambipolar characteristics; diode-like curves at low gate bias and saturation curves at high gate bias. These features occur because of the presence of both hole and electron charge carriers in the same

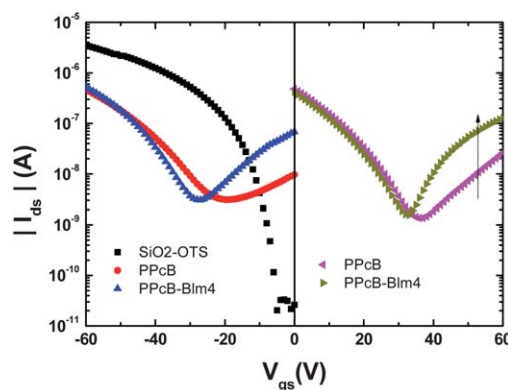


**Fig. 2** Transport characteristic curves of PCDTBT FETs.

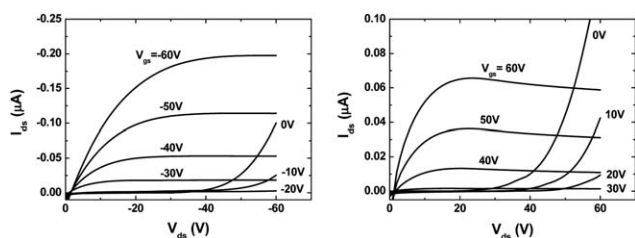


Fig. 3 Output characteristic curves of a PCDTBT ambipolar FET fabricated on a PPcB layer.

channel. At high gate voltages, true p- or n-channel behavior begins to appear.

Self-assembled monolayer (SAM) treatment of a SiO<sub>2</sub> gate dielectric using OTS also can be a good way to remove interfacial traps. However, SAM using OTS cannot completely eliminate surface hydroxyl groups. There has been a report that stable n-channel conduction was observed in fully conjugated aromatic polymers when polyethylene (PE) or a divinyltetramethylsiloxane-bis(benzocyclobutene) (BCB) derivative was used as the buffer dielectric.<sup>20</sup> In such cases, however, Ca was used as the source-drain electrode to inject electrons. In our FET devices, n-type behavior was clearly observed with Au source-drain electrodes, even though there was a large electron injection barrier. This result indicated that there is a certain energy band structure change in the active polymer on the PPcB layer.

We used ultraviolet photoelectron spectroscopy (UPS) to elucidate changes in the energy band structure. Fig. 4 displays the UPS spectra taken from PCDTBT and PPcB/PCDTBT films. The shape of the UPS spectrum of PCDTBT agrees well with results from a previous report.<sup>23</sup> All spectra were plotted with respect to the Fermi level ( $E_F$ ) of Au. The normalized secondary cutoff edges of PCDTBT and PPcB/PCDTBT films are shown in the left panel of Fig. 4. The vacuum levels of the samples were determined by linear extrapolation of secondary electron cutoffs on the high-binding energy side of the UPS spectra (14–19 eV). The vacuum level shifted by *ca.* 0.32 eV toward a higher binding energy after PPcB deposition compared to that of the bare PCDTBT film, thus indicating the presence of an interface dipole, as previously reported.<sup>21</sup> The right panel of Fig. 4 shows HOMO onset positions for the PCDTBT and PPcB/PCDTBT

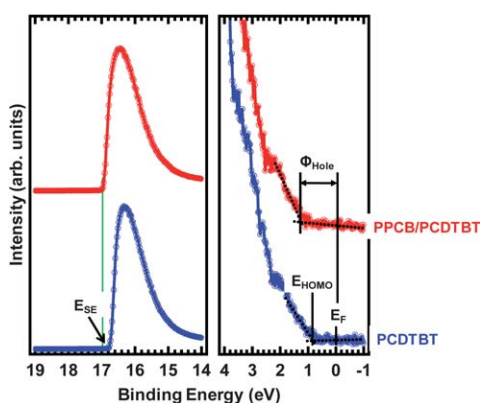


Fig. 4 Ultraviolet photoelectron spectroscopy (UPS) spectra taken from PCDTBT and PPcB/PCDTBT films.

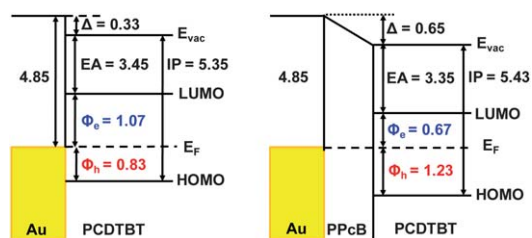


Fig. 5 The schematic energy level diagrams of PCDTBT and PPcB/PCDTBT interfaces.

films. The HOMO onset positions were at 0.83 eV for PCDTBT and 1.23 eV for PPcB/PCDTBT below  $E_F$ .

Vacuum levels and HOMO onset positions are summarized in the schematic energy level diagrams of PCDTBT and PPcB/PCDTBT interfaces, as shown in Fig. 5. The LUMO energies were estimated using the HOMO level and the optical gap ( $E_g = 1.9$  eV for PCDTBT) with the uncertainty of exciton binding energy.<sup>24</sup> The value between  $E_F$  and the LUMO level is also frequently used as a measure of the electron injection barrier ( $\phi_e$ ). The PPcB layer reduced the  $\phi_h$  by 0.40 eV, from 1.07 eV to 0.67 eV, compared to that of the PCDTBT. Even though the specific mechanisms related to the charge injection efficiency might be complex, it is clear that the smaller  $\phi_e$  contributes to the efficient electron transport of OFETs. The UPS results indicate that the PPcB layer causes a downward shift in the vacuum level, thereby decreasing the LUMO energy and the reduction in  $\phi_e$  as shown in Fig. 5.

In order to determine if the effect of the PPcB layer is a general phenomenon, we have explored the ambipolar behavior for other types of D–A conjugated copolymers. Note that all D–A conjugated copolymers tested in this study were generally considered p-type semiconductors. Fig. 6 shows the transport characteristics of bipolar FET using poly(5,6-bis(octyloxy)-4-(thiophen-2-yl)benzo[*c*]-1,2,5-thiadiazole) (PTBT) and poly[(4,4'-bis(2-ethylhexyl)dithiophene[3,2-*b*:2',3'-*d*]silole)-2,6-diyl-*alt*-(4,7-bis(2-thienyl)-2,1,3-benzothiadiazole)-5,5'-diyl] (Si-PCPDtBT) fabricated on a

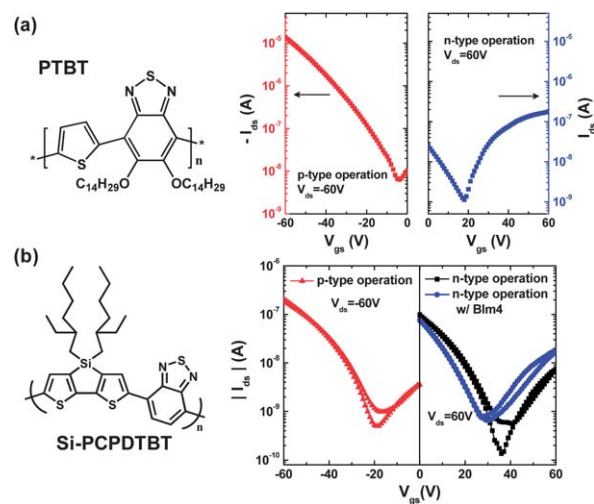


Fig. 6 (a) Transport characteristics of bipolar FET using PTBT fabricated on a PPcB layer. (b) Transport characteristics of bipolar FET using Si-PCPDtBT fabricated on a PPcB layer.

PPcB layer. In the case of PTBT, the FET device with OTS treatment showed only p-type behavior (see Fig. S2 in the ESI†). However, the device with the PPcB layer showed clear ambipolar behavior. The measured hole mobility was  $6.7 \times 10^{-2} \text{ cm}^2 \text{ V}^{-1} \text{ s}^{-1}$  and the electron mobility was  $1.3 \times 10^{-2} \text{ cm}^2 \text{ V}^{-1} \text{ s}^{-1}$ . For the Si-PCPDTBT, typical ambipolar characteristics were apparent with the PPcB layer. Similar to the PCDTBT case, insertion of the Blm4 electron injection layer between the active layer, Au source and drain electrodes enhanced electron injection properties, thereby slightly improving the n-type behavior. Si-PCPDTBT ambipolar FETs exhibited hole and electron mobilities of  $1.7 \times 10^{-3} \text{ cm}^2 \text{ V}^{-1} \text{ s}^{-1}$  and  $1.1 \times 10^{-4} \text{ cm}^2 \text{ V}^{-1} \text{ s}^{-1}$ , respectively. The output characteristics of PTBT and Si-PCPDTBT ambipolar FETs are presented in the ESI.†

## Conclusions

We observed ambipolar properties of a D–A-conjugated copolymer by introducing a PPcB functional layer between the SiO<sub>2</sub> insulating layer and the active polymer layer. We explored three different copolymers, PCDTBT, PTBT and Si-PCPDTBT, generally considered to be p-type semiconductors. All copolymers showed typical p-type characteristics with an OT-treated SiO<sub>2</sub> substrate. However, with the PPcB passivation layer, clear ambipolar characteristics were observed. The PPcB layer effectively covered the hydroxyl groups which acted as trap sites for electrons and induced a reduction in the energetic disorder at the semiconductor–insulator interface. As a result, the FET devices fabricated using D–A conjugated copolymers showed clear ambipolar properties.

## Acknowledgements

This work was supported by the Research Fund of the University of Ulsan.

## Notes and references

1 A. M. C. Scharber, D. Mühlbacher, M. Koppe, P. Denk, C. Waldauf, A. J. Heeger and C. J. Brabec, *Adv. Mater.*, 2006, **18**, 789–794.

- 2 S. H. Park, A. Roy, S. Beaupré, S. Cho, N. Coates, J. S. Moon, D. Moses, M. Leclerc, K. Lee and A. J. Heeger, *Nat. Photonics*, 2009, **3**, 297–302.
- 3 N. Blouin, A. Michaud and M. Leclerc, *Adv. Mater.*, 2007, **19**, 2295–2300.
- 4 H.-Y. Chen, J. Hou, S. Zhang, Y. Liang, G. Yang, Y. Yang, Y. L. Yu, Y. Wu and G. Li, *Nat. Photonics*, 2009, **3**, 649–653.
- 5 R. C. Coffin, J. Peet, J. Rogers and G. C. Bazan, *Nat. Chem.*, 2009, **1**, 657–661.
- 6 Y.-C. Chen, C.-Y. Yu, Y.-L. Fan, L.-I. Hung, C.-P. Chen and C. Ting, *Chem. Commun.*, 2010, **46**, 6503–6505.
- 7 J. Peet, J. Y. Kim, N. E. Coates, W. L. Ma, D. Moses, A. J. Heeger and G. C. Bazan, *Nat. Mater.*, 2007, **6**, 497–500.
- 8 J. Kim, S. H. Kim, I. H. Jung, E. Jeong, Y. Xia, S. Cho, I.-W. Hwang, K. Lee, H. Suh, H.-K. Shim and H. Y. Woo, *J. Mater. Chem.*, 2010, **20**, 1577–1586.
- 9 S. Cho, J. H. Seo, S. H. Park, S. Beaupré, M. Leclerc and A. J. Heeger, *Adv. Mater.*, 2010, **22**, 1253–1257.
- 10 C. Yang, S. Cho, R. C. Chiechi, W. Walker, N. E. Coates, D. Moses, A. J. Heeger and F. Wudl, *J. Am. Chem. Soc.*, 2008, **130**, 16524–16526.
- 11 E. S. H. Kang, J. D. Yuen, W. Walker, N. E. Coates, S. Cho, E. Kim and F. Wudl, *J. Mater. Chem.*, 2010, **20**, 2759–2765.
- 12 J. Lee, S. Cho and C. Yang, *J. Mater. Chem.*, 2011, **21**, 8528–8531.
- 13 S. K. Lee, S. Cho, M. Tong, J. H. Seo and A. J. Heeger, *J. Polym. Sci., Part A: Polym. Chem.*, 2011, **49**, 1821–1829.
- 14 J. S. Ha, K. H. Kim and D. H. Choi, *J. Am. Chem. Soc.*, 2011, **133**, 10364–10367.
- 15 H. N. Tsao, D. M. Cho, I. Park, M. R. Hansen, A. Mavrinskiy, D. Y. Yoon, R. Graf, W. Pisula, H. W. Spiess and K. Müllen, *J. Am. Chem. Soc.*, 2011, **133**, 2605–2612.
- 16 J. D. Yuen, R. Kumar, D. Zakhidov, J. Seifter, B. Lim, A. J. Heeger and F. Wudl, *Adv. Mater.*, 2011, **23**, 3780–3785.
- 17 S. Cho, J. Lee, M. Tong, J. H. Seo and C. Yang, *Adv. Funct. Mater.*, 2011, **21**, 1910–1916.
- 18 H. S. Oh, T.-D. Kim, Y.-H. Koh, K.-S. Lee, S. Cho, A. Cartwright and P. N. Prasad, *Chem. Commun.*, 2011, **47**, 8931–8933.
- 19 J. D. Yuen, J. Fan, J. Seifter, B. Lim, R. Hufschmid, A. J. Heeger and F. Wudl, *J. Am. Chem. Soc.*, 2011, **133**, 20799–20807.
- 20 L.-L. Chua, J. Zaumseil, J.-F. Chang, E. C.-W. Ou, P. K.-H. Ho, H. Sirringhaus and R. H. Friend, *Nature*, 2005, **434**, 194–199.
- 21 J. H. Seo and T.-Q. Nguyen, *J. Am. Chem. Soc.*, 2008, **130**, 10042–10043.
- 22 J. H. Seo, A. Gutacker, B. Walker, S. Cho, A. Garcia, R. Yang, T.-Q. Nguyen, A. J. Heeger and G. C. Bazan, *J. Am. Chem. Soc.*, 2009, **131**, 18220–18221.
- 23 J. H. Seo, S. Cho, M. Leclerc and A. J. Heeger, *Chem. Phys. Lett.*, 2011, **503**, 101–104.
- 24 J. H. Seo, Y. Jin, J. Z. Brzezinski, B. Walker and T.-Q. Nguyen, *ChemPhysChem*, 2009, **10**, 1023–1027.